



## Low temperature aging effects on the formation of Sn nanoclusters in SiO<sub>2</sub>/Si films and interfaces

Felipe Kremer, João M. J. Lopes, Fernando C. Zawislak, and Paulo F. P. Fichtner

Citation: [Applied Physics Letters](#) **91**, 083102 (2007); doi: 10.1063/1.2772236

View online: <http://dx.doi.org/10.1063/1.2772236>

View Table of Contents: <http://scitation.aip.org/content/aip/journal/apl/91/8?ver=pdfcov>

Published by the [AIP Publishing](#)

---

### Articles you may be interested in

[Effects of surface oxide layer on nanocavity formation and silver gettering in hydrogen ion implanted silicon](#)  
J. Appl. Phys. **114**, 023502 (2013); 10.1063/1.4812736

[Aging effects on the nucleation of Pb nanoparticles in silica](#)  
J. Appl. Phys. **109**, 014320 (2011); 10.1063/1.3530844

[Effects of low-fluence swift iodine ion bombardment on the crystallization of ion-beam-synthesized silicon carbide](#)  
J. Appl. Phys. **101**, 084311 (2007); 10.1063/1.2720090

[Introduction of Si/SiO<sub>2</sub> interface states by annealing Ge-implanted films](#)  
J. Appl. Phys. **96**, 4308 (2004); 10.1063/1.1790579

[Thermal stability of SiO<sub>2</sub> / CoSi<sub>2</sub> / polysilicon multilayer structures improved by cavity formation](#)  
J. Vac. Sci. Technol. B **20**, 880 (2002); 10.1116/1.1475681

---

The image shows the cover of an Applied Physics Reviews journal issue. It features a blue and orange color scheme with a molecular structure background. The text 'NEW Special Topic Sections' is prominently displayed in white. Below it, 'NOW ONLINE' is written in yellow, followed by the title 'Lithium Niobate Properties and Applications: Reviews of Emerging Trends' in white. The AIP Applied Physics Reviews logo is in the bottom right corner.

**NEW Special Topic Sections**

**NOW ONLINE**  
Lithium Niobate Properties and Applications:  
Reviews of Emerging Trends

**AIP** Applied Physics  
Reviews

## Low temperature aging effects on the formation of Sn nanoclusters in SiO<sub>2</sub>/Si films and interfaces

Felipe Kremer, João M. J. Lopes,<sup>a)</sup> and Fernando C. Zawislak  
*Instituto de Física, UFRGS, 91501-970 Porto Alegre, Brazil*

Paulo F. P. Fichtner<sup>b)</sup>  
*Escola de Engenharia, UFRGS, 91501-970 Porto Alegre, Brazil*

(Received 11 April 2007; accepted 25 July 2007; published online 21 August 2007)

The formation of Sn nanocrystals (NCs) in ion implanted SiO<sub>2</sub>/Si films is investigated using Rutherford backscattering spectrometry and transmission electron microscopy. Low temperature and long time aging treatments followed by high temperature thermal annealings lead to the formation of a dense bidimensional NC array located at the SiO<sub>2</sub>/Si interface. This behavior is discussed considering the formation of small Sn clusters with a significantly improved thermal stability. The present experimental results are in good agreement with recent theoretical predictions that small Sn clusters can have their melting temperature enhanced in more than 1000 °C.

© 2007 American Institute of Physics. [DOI: 10.1063/1.2772236]

The formation of dense arrays of functional nanocrystals (NCs) in silicon oxide films is of great interest for several applications within the information technology context. This comprises, e.g., data storage based on their electric properties,<sup>1,2</sup> data transmission based on photonic or plasmonic behavior,<sup>3,4</sup> or even data processing in terms of single electron devices.<sup>5,6</sup> Dense arrays of NCs can be produced inside thin films, e.g., by means of ion implantation or via codeposition of the film and the NC elements, followed by high temperature thermal treatments. In order to tailor their size and space distribution, it is important to understand the structure evolution involving the NC formation in SiO<sub>2</sub> films, from the atomic scale deposition or implantation processes to their final structure, shape, size, and spatial distributions. For room temperature ion implanted silica films with ion fluences  $\phi \geq 1 \times 10^{16} \text{ cm}^{-2}$ , it is generally accepted that nanoparticle embryos may form during the implantation. However, depending on the mobility and chemical reactivity of the implanted ion species, stable NCs may be obtained only upon postimplantation thermal treatments.

In this letter, we will focus on the thermal behavior of Sn<sup>+</sup> implanted SiO<sub>2</sub> films presenting a specific phase segregation phenomenon capable to induce significant modifications in the thermal evolution of the microstructure. The structural characteristics of Sn implanted silica have been previously studied as a function of the annealing temperature and atmosphere. Thermal treatments under high vacuum result in more uniform and homogeneously distributed nanoparticle systems,<sup>7</sup> while annealings under N<sub>2</sub> flux preferentially result in layered structures containing NCs of quite distinct sizes and phases, including NC structures presenting a metallic  $\beta$ -Sn core and a polycrystalline Sn-O shell.<sup>7,8</sup> In addition, as demonstrated by Spiga *et al.*,<sup>9</sup> the chemical reactivity of the Sn atoms seems to be also important. In as-implanted silica, the Sn atoms are preferentially coordinated with oxygen. Such a Sn-O coordination remains up to an-

nealing temperatures  $T \leq 900 \text{ °C}$  and times  $t \leq 30 \text{ s}$ . For higher temperatures or longer times, the formation of  $\beta$ -Sn NCs takes place. In the present work, we show that, on specific two step thermal treatment conditions, it is possible to modify significantly the above scenario describing the formation of NCs in Sn<sup>+</sup> implanted silica films. As a limit situation, we demonstrate that the formation of stable Sn-based NCs inside the films can be suppressed even for implanted fluences of  $2 \times 10^{16} \text{ cm}^{-2}$  and annealing temperatures and times as high as 1100 °C during 6 h. This behavior introduces a higher level of control for the sophisticated microstructure designs already obtained in Sn<sup>+</sup> implanted and high temperature annealed silica films.<sup>7,10</sup> One of the consequences demonstrated here is the exclusive formation of a dense and bidimensional array of metallic  $\beta$ -Sn NCs located at the SiO<sub>2</sub>/Si(100) interface. The present observations are discussed in terms of a nanoscale phenomenon considering the enhancement of the thermal stability predicted for small Sn clusters.<sup>11,12</sup>

250 nm thick SiO<sub>2</sub> films were thermally grown on n-type Si(100) wafers in a wet ambient at 1000 °C. The films were implanted with Sn ions at 300 keV and fluences from 1.7 to  $2 \times 10^{16} \text{ cm}^{-2}$  Sn. This combination of energy and fluence produces a Gaussian-like Sn concentration-depth profile centered in the middle of the SiO<sub>2</sub> layer, with peak concentrations of  $\approx 3 \text{ at. } \%$ . Postimplantation thermal treatments were performed in a conventional high vacuum furnace considering either one or two process steps. The single step treatments were performed in a pressure of  $\approx 10^{-6} \text{ mbar}$  at 1100 °C for distinct times from 0.5 to 6 h. The two step processes were performed considering first a low temperature aging in air step [from 25 (RT) to 250 °C] and longer times (from 1 day to 1 yr, i.e.,  $\approx 8700 \text{ h}$ ), followed by a high temperature treatment also at 1100 °C for 0.5–6 h in  $\approx 10^{-6} \text{ mbar}$ . The concentration distribution depth profile of the implanted Sn atoms, before and after the annealings, has been characterized by Rutherford backscattering spectrometry using 1 MeV  $\alpha$  particles. The transmission electron microscopy (TEM) observations were performed at 200 kV in cross-sectional and plan-view samples prepared by ion milling.

<sup>a)</sup>Present address: Institute for Bio- and Nanosystems (IBNI-IT), Research Center Jülich, Germany.

<sup>b)</sup>Author to whom correspondence should be addressed; also at Laboratório de Implantação Iônica, Instituto de Física, UFRGS, Porto Alegre, Brazil; electronic mail: paulo.fichtner@ufrgs.br

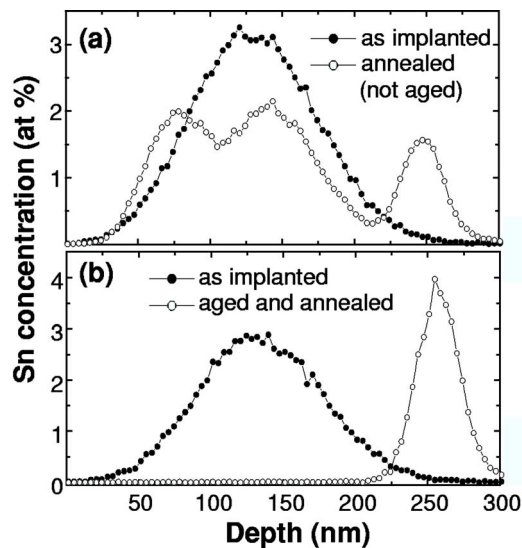


FIG. 1. RBS measurements of  $\text{Sn}^+$  implanted  $\text{SiO}_2/\text{Si}$ . The full circles stand for the as-implanted samples and the open ones for samples annealed for 6 h at  $1100^\circ\text{C}$  in high vacuum. (a) Sample implanted with the fluence of  $2 \times 10^{16} \text{ cm}^{-2}$  Sn and directly annealed. (b) Sample implanted with the fluence of  $1.7 \times 10^{16} \text{ cm}^{-2}$  Sn, aged during 1 yr at  $25^\circ\text{C}$  in air and then annealed. The peaks located at the depth of  $\approx 250 \text{ nm}$  represent the Sn content at the  $\text{SiO}_2/\text{Si}$  interface.

Figure 1 shows the Rutherford backscattering spectrometry (RBS) measurements of as-implanted and thermally annealed samples. Figure 1(a) corresponds to a case where as-implanted samples were treated directly at  $1100^\circ\text{C}$  for 6 h. The evaluation of the Sn signal shows that a fraction of  $\approx 18\%$  of the implanted Sn atoms redistributes and forms a sharp peak at the interface and  $\approx 7\%$  of the total Sn content is lost by evaporation. It also shows that  $\approx 75\%$  of the Sn content remains inside the silica film, thus leading to the formation of  $\beta$ -Sn NC with distinct arrangements depending on the annealing temperature and atmosphere as demonstrated previously.<sup>7,13</sup> Figure 1(b) shows that two step processes, consisting of a 1 yr aging treatment in air at room temperature ( $25^\circ\text{C}$ ) followed by a  $1100^\circ\text{C}$  annealing in high vacuum for 6 h, lead to very different results: a fraction ( $\approx 35\%$ ) of the implanted Sn content has accumulated at the  $\text{SiO}_2/\text{Si}(100)$  interface and the remaining Sn has been lost by evaporation. Within the sensitivity of the RBS measurements, the silica film becomes free of Sn atoms. Figure 2(a) shows a cross-section TEM image from the same sample, as in Fig. 1(b). The Sn atoms have agglomerated forming the NCs located at the interface. A careful TEM inspection of the  $\text{SiO}_2$  film did not show voids and or any additional particle inside the silica film. The NCs present a lenticular shape [Fig. 2(b)], half embedded inside the Si substrate. These lenticular structures have rather regular heights with a mean value of  $\approx 12.2 \text{ nm}$  and a standard deviation  $\sigma \approx 3.2 \text{ nm}$ . Figure 2(c) shows a plan-view image of the overall NC planar arrangement. The smaller particles present a squarelike shape while the larger ones tend to become more circular. Their lateral size distribution is shown in Fig. 2(d). The overall particle concentration is  $\approx 6 \times 10^{10} \text{ cm}^{-2}$ ; the size distribution is monomodal with mean characteristic diameters of  $\approx 20 \text{ nm}$  and standard deviation  $\sigma \approx 4.4 \text{ nm}$ . Selected area diffraction patterns (not shown) demonstrate that the particles are of the  $\beta$ -Sn (metallic) phase, presenting distinct orientations with respect to the Si matrix.

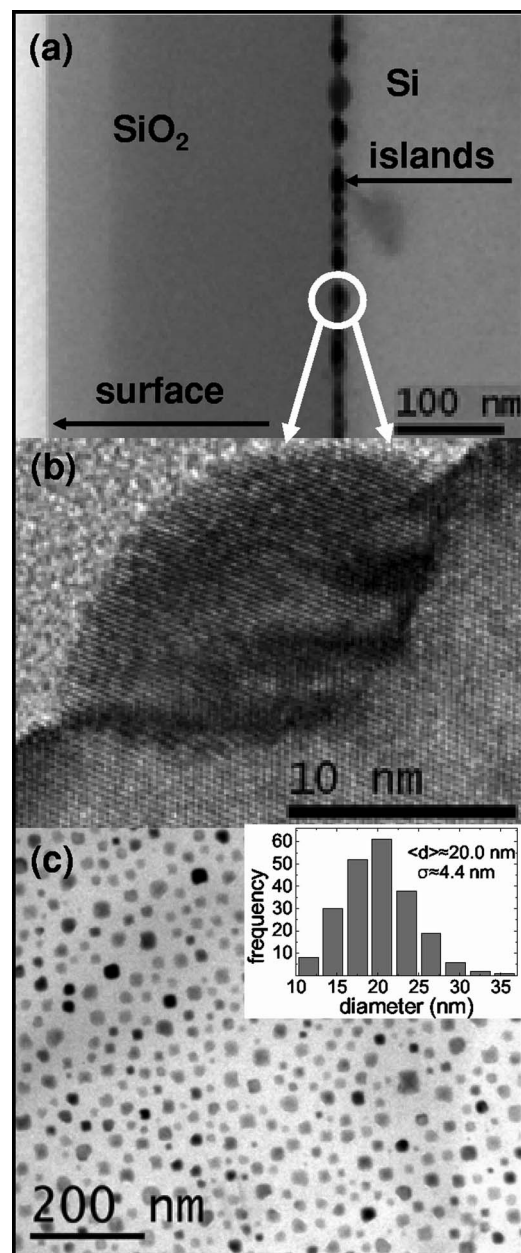


FIG. 2. TEM micrographs presenting (a) cross-section image showing the Sn nanoclusters at the  $\text{SiO}_2/\text{Si}(100)$  interface and the  $\text{SiO}_2$  film free of TEM detectable particles, (b) enlarged cross-sectional view from an interface cluster showing its crystalline arrangement and its lenticular shape half embedded in the Si matrix, and (c) plan-view image from the interface region showing the cluster arrangement. The inset shows their size distribution histogram (characteristic diameters).

In order to get more insight into this evolutionary behavior taking place during the two step thermal treatments, we have tested the Sn redistribution characteristics considering 100 h aging treatments in air at distinct temperatures ( $75$ ,  $150$ , and  $250^\circ\text{C}$ ), followed by a 6 h long second step treatment at  $1100^\circ\text{C}$  in  $\approx 10^{-6}$  mbar. The RBS measurements shown in Fig. 3 demonstrate that the total quantity of Sn atoms remaining inside the silica film decreases with the increase of the aging temperature. This occurs as the Sn atoms evaporate at the free surface or redistribute forming NCs at the  $\text{SiO}_2/\text{Si}$  interface. For the aging temperature of  $250^\circ\text{C}$ , the evaporation losses correspond to  $\approx 54\%$  of the total implanted content, while a fraction  $\approx 42\%$  has redistributed to the interface, and  $\approx 4\%$  still remains inside the silica



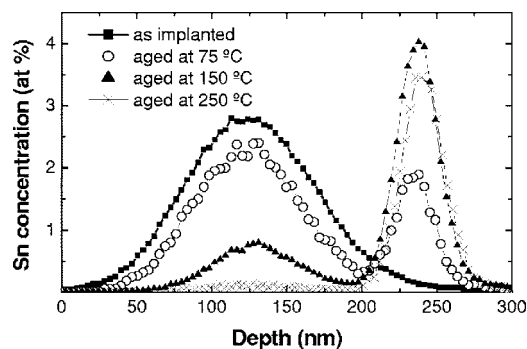


FIG. 3. RBS measurements of Sn concentration-depth profile considering aging treatments in air during 100 h at distinct temperatures. After the aging, the samples were annealed for 6.0 h at 1100 °C in high vacuum. The profile of an as-implanted sample is also shown as a reference curve.

film. The maximum Sn fraction at the interface region is observed for the aging temperature of 150 °C, corresponding to  $\approx 46\%$  of the implanted content, however, with a larger Sn fraction (19%) remaining inside the silica film.

The above results show that the low temperature aging treatment is a crucial step significantly affecting the microstructure evolution of the  $\text{Sn}^+$  implanted silica films. As previously reported by different groups,<sup>8,9,13</sup> classical nucleation concepts can explain the formation of nanoparticles inside silica, as commonly obtained via a one step thermal treatment. In this sense, observed losses of the implanted content usually occur at rather high temperatures ( $T > 900$  °C), and can be related to the dissolution of larger particles, which show additional void contrast clearly observed by TEM (not shown) as their Sn content diminishes.

In the case of the Sn implanted samples aged for 1 yr at room temperature [Fig. 2(a)], we have not detected the presence of voids or any additional particles inside the silica. Hence, the major effect of the aging treatment seems to be the formation of embryos or small Sn clusters, very probably due to the limited mobility of the Sn atoms at the low aging temperatures. Upon thermal treatments at higher temperatures, the absence of voids or any other particles leads to the assumption that particle coarsening did not occur, even at temperatures as high as 1100 °C for 6 h long treatments. As a consequence, it is necessary to postulate that the small Sn clusters have acquired an enhanced thermal stability and only began to slowly dissociate at temperatures close to 1100 °C. Indeed, this assumption is supported by recent experimental<sup>14,15</sup> and theoretical<sup>11,12</sup> findings. It has been demonstrated that Sn clusters with 5–20 atoms can present an enhanced thermal stability and, as opposed to most of nanoparticle systems, may lead to a significant increase of their melting point as compared to the bulk value. First principles calculations show that the melting point of  $\text{Sn}_{10}$  or  $\text{Sn}_{20}$  clusters may reach temperatures as high as 1100–1300 °C. The drastic increase of melting temperatures was explained as a nanoscale phenomenon resulting from the preferential formation of covalent bonds and a specific atomic structure, typically trigonal triangular prisms, instead of metallic close packed ones. This predicted property of such small Sn clusters could explain our results. Their formation may require very long times (of the order of 1 yr) at RT. For shorter aging times such as 100 h at 75, 150, or 250 °C, the fraction of stable clusters seems to increase with the aging temperature as the mobility of the Sn atoms also increases. Because of their enhanced thermal stability, the

clusters may only start to dissolve at a sufficiently high temperature (in our case 1100 °C). Hence, the release rate of the Sn atoms from the small clusters is slow as compared to the atomic diffusivity, and therefore classical nucleation is inhibited since the formation of clusters with large critical radius value becomes improbable. Thus, as the Sn atoms dissociate from the small clusters, they are free to diffuse, redistributing toward sinks represented by the free surface (leading to losses by evaporation), by the interface or even by the Si matrix as Sn becomes more soluble at temperatures around 1060 °C.<sup>16</sup> This situation can lead to heterogeneous nucleation of nanoparticles at the interface, as discussed previously.<sup>13</sup>

In summary, we have demonstrated that aging treatments in Sn implanted silica provide an alternative method to nanostructure silica films and  $\text{SiO}_2/\text{Si}$  interfaces. In particular, we demonstrate that the formation of Sn rich nanoclusters in ion implanted silica films can be inhibited, leading to the exclusive formation of a bidimensional and dense arrangement of rather uniform nanoclusters at the  $\text{SiO}_2/\text{Si}$  interface. This phenomenon was discussed considering the formation of highly stable small Sn clusters, contradicting the usual concept that the thermal stability decreases with the nanoclusters size. The present results are consistent with recent theoretical predictions and may represent the first experimental confirmation that the thermal stability of small Sn clusters can be significantly enhanced in  $\approx 1000$  °C.

The authors acknowledge the use of the facilities of CME-UFRGS and the support from CAPES, CNPq, FAPERGS, and FINEP. Two of the authors (P.F.P.F. and J.M.J.L.) also acknowledge the support from the AvH Foundation, Germany.

<sup>1</sup>R. J. Walters, P. G. Kik, J. D. Casperson, H. A. Atwater, R. Lindsted, M. Giorgi, and G. Bourianoff, *Appl. Phys. Lett.* **85**, 2622 (2004).

<sup>2</sup>P. Dimitrakis, E. Kapenatakis, D. Tsoukalas, D. Skarlatos, C. Bonafos, G. Bem Assayag, A. Claverie, M. Perego, M. Fanciulli, V. Soncini, R. Sotgiu, A. Agarwal, M. Ameen, C. Sohl, and P. Normand, *Solid-State Electron.* **48**, 1511 (2004).

<sup>3</sup>Y. Xin and N. J. Hallas, *MRS Bull.* **30**, 328 (2005).

<sup>4</sup>S. A. Mayer, and H. A. Atwater, *J. Appl. Phys.* **98**, 011101 (2005).

<sup>5</sup>W. Chen and H. Ahmed, *J. Vac. Sci. Technol. B* **15**, 1402 (1997).

<sup>6</sup>T. Kubota, T. Hashimoto, Y. Ishikawa, S. Samukawa, A. Miura, Y. Uraoka, T. Fuyuki, M. Takeguchi, K. Nishioka, and I. Yamashita, *Appl. Phys. Lett.* **89**, 233127 (2006).

<sup>7</sup>J. M. J. Lopes, F. C. Zawislak, P. F. P. Fichtner, F. C. Lovey, and A. M. Condó, *Appl. Phys. Lett.* **86**, 023101 (2005).

<sup>8</sup>A. Markvitz, R. Grötzschel, K. H. Heinig, L. Rebohle, and W. Skorupa, *Nucl. Instrum. Methods Phys. Res. B* **152**, 319 (1999).

<sup>9</sup>S. Spiga, R. Mantovan, M. Fanciulli, N. Ferreti, F. Boscherini, F. d'Acapito, B. Schimidt, R. Grötzschel, and A. Mücklich, *Phys. Rev. B* **68**, 205419 (2003).

<sup>10</sup>A. Nakajima, T. Futatsugi, H. Nakao, T. Usuki, N. Horigushi, and N. Yokohama, *J. Appl. Phys.* **84**, 1316 (1998).

<sup>11</sup>K. Joshi, D. G. Kanhere, and S. A. Blundell, *Phys. Rev. B* **67**, 235413 (2003).

<sup>12</sup>F. Chuang, C. Z. Wang, S. Ögüt, J. R. Chelikowsky, and K. M. Ho, *Phys. Rev. B* **69**, 165408 (2004).

<sup>13</sup>J. M. J. Lopes, F. C. Zawislak, P. F. P. Fichtner, R. M. Papaléo, F. C. Lovey, A. M. Condó, and A. J. Tolley, *Appl. Phys. Lett.* **86**, 191914 (2005).

<sup>14</sup>A. A. Shvartsburg, and M. F. Jarrold, *Phys. Rev. Lett.* **85**, 2530 (2000).

<sup>15</sup>Q. Xu, I. D. Sharp, C. W. Yuan, D. O. Yi, C. Y. Liao, A. M. Gleaser, A. M. Minor, J. W. Beeman, M. C. Ridgway, P. Kluth, J. W. Ager III, D. C. Chrzan, and E. E. Haller, *Phys. Rev. Lett.* **97**, 155701 (2006).

<sup>16</sup>R. W. Olesinski and G. J. Abbaschian, in *Binary Alloy Phase Diagrams*, 2nd ed., edited by T. B. Massalski (ASM International, Ohio, 1992), Vol. 3, p. 3362.